Time-Accurate Simulation of Aeroelastic Flap Deployment with Free Play

Nicolas D. Reveles,[*] George Antoun,[*] James Fort[+]

[*]ATA Engineering, Inc.

[+]Dassault Systems Simulia Corp.

***Abstract**: Today, numerous aeroelastic structures are deployed over a finite time period, such as flaps, spoilers, control surfaces, and wheel bay and bomb bay doors. These devices must be both divergence and flutter free. Current state-of-art simulations verify this by applying a quasi-steady assumption that does not require the system to physically deploy within the computations. That is, the structure is assumed elastic but does not possess the "large" motion associated with the device's path of travel. While these simulations have strong technical merit, especially in the case where a structure is inadvertently locked in a partially deployed position, they are unable to capture all of the relevant physics. When a component is deployed over a finite period, the flow physics include additional unsteady aerodynamic effects that are lost without considering the large motion of the device; in addition to the unsteady aerodynamics, the structure has inertial terms that cannot be correctly accounted for with the quasi-steady assumption. It will be demonstrated that by coupling Abaqus/Standard, which simulates the elastic response and flexible multibody dynamic articulation, to the CFD solver Star-CCM+ via Simulia's Co-Simulation Engine (CSE), a time-accurate response to flap deployment can be achieved. This is compared to results from a simulation utilizing the quasi-steady assumption.*

***Keywords**: Aeroelasticity, CFD Coupling, Connectors, Coupled Analysis, Dynamics, Elasticity, Flap, Free Play, Multi-Body Dynamics*

1. Introduction

The determination of the aeroelastic response of deployable structures is a challenging but necessary multidisciplinary task. Common structures such as flaps, spoilers, control surfaces, and wheel bay and bomb bay doors all contain multiple configurations that require actuators to deploy. These different configurations may have substantially different aerodynamic effects acting on them between the fully deployed and withdrawn positions due to the possibilities of vortex shedding, separation, and stall. These nonlinear aerodynamic phenomena are responsible for determining the structure's aeroelastic stability margin, the structural loads, and the actuator force required for timely deployment.

Modern aeroelastic analyses accomplish this by examining the structural response of the part at a fixed deployment angle to computed aerodynamic loading (Blades & Cornish, January, 2015). To accurately model the nonlinear effects of the aerodynamic loading, the unsteady Reynolds-averaged Navier–Stokes (URANS) equations are typically resolved on a computational mesh.

These equations allow for the efficient solution of the fluid dynamics by modeling the turbulence rather than resolving it. The URANS equations may become inappropriate in situations where large separated flow exists and the turbulent time scales begin to approach the unsteady flow time scales. Large-eddy simulation (LES) enables resolution of these large turbulent scales while still modeling the fine-scale turbulence; however, it does so at greatly increased computational costs that may not be suitable for engineering-level analyses today. On the other hand, detached-eddy simulation (DES) is a hybrid approach especially suitable for separated flows. With DES, the URANS equations provide closure in regions where the mesh is too coarse to resolve the largest turbulent eddies (e.g., boundary layers), and LES computations are performed in refined regions where the turbulent scales may be captured (e.g., separated flow on a fine mesh).

The physical motion of the part itself may induce unsteady aerodynamic effects that modify aeroelastic stability margins. With the addition of the structural inertial terms, it is possible that the dynamic response of the deployment may be significantly different from the quasi-static response to the elastic structure held at a fixed deployment angle.

One challenge in solving CFD problems with large relative motion is how to best represent the moving domains. Today, the so-called "chimera" or overset approach (Mitcheltree, et al., 1988) is most commonly employed in these situations. This technique allows multiple overlapping grids to define the domain of interest. When the meshes are moving, at each time step several steps must occur: holes are cut in any mesh that overlaps a body, and mesh fringe points are identified and marked as "donors" and "receivers," depending on whether they are used to interpolate to or from another mesh, respectively. Finally, the fringe points are updated as an overset boundary condition. For simulations with large relative motion, such as rotorcraft, the overset approach is an enabling technology (Noack, June 2007).

Overset methods can be employed to account for the large motion of articulating bodies such as flap deployments or bay door motions; however, these problems can be further complicated by the mechanical wearing of parts over their lifetime that introduces an element of free play. This free play allows some limited amount of unrestrained motion around the commanded position so that the exact position of the motion body cannot be precisely controlled. Free play has been recognized as an important parameter to consider in the aeroelastic analyses of components. The FAA Advisory Circular 25.629 section 6.3.4 (Federal Aviation Administration, October 2014) states, "Consideration of free play may be incorporated as a variation in stiffness to assure adequate limits are established for wear of components such as control surface actuators, hinge bearings, and engine mounts in order to maintain aeroelastic stability margins." It also states in section 7.1.4.1 that "Freeplay effects should be incorporated to account for any influence of in-service wear on flutter margins," as well as that "Once the analysis has been conducted with the nominal, experimentally adjusted values of hinge moment coefficients, the analysis should be conducted with parametric variations of the coefficients and other parameters subject to variability." Therefore, it is ideal to create a system model that enables incremental changes to the free play to examine the effects and understand required tolerances.

When the aerodynamic response may be considered linear, it is possible to develop theoretical mathematical models that describe the system (Tang & Dowell, November 2011). However, when incorporating free play into aeroelastic analyses of deployable structures subject to nonlinear aerodynamics, such models are not readily constructed. It is the intent of this paper to demonstrate

how these effects can be accounted for at reasonable computational expense through the use of commercially available software packages. This will be demonstrated using a notional example of an elastic flap deploying behind an elastic slat where the flap contains various amounts of free play.

2. Demonstration Case

The demonstration case considered is depicted in Figure 1. The flap is designed to deploy by sliding aft while simultaneously rotating into the flow at a positive angle of attack. Computations were performed to approximately 18° (illustrated in Figure 2), past where stall and separation begin. The actuation was analyzed with ±1° of free play as well as with no free play.

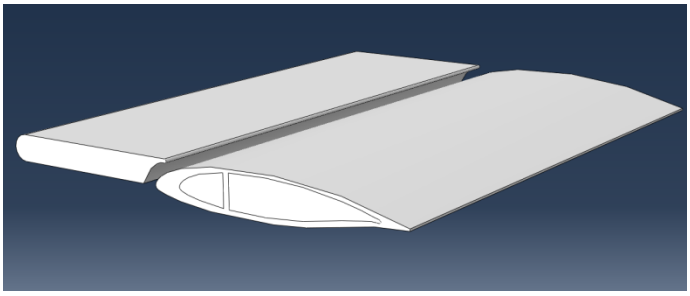

Figure 1. The geometry of the case considered consists of a leading slat and a trailing flap.

Figure 2. Three commanded deployment angles for the slat/flap system are depicted: 0°, 10°, and 18°.

The notional flap geometry is made of a modified Wortmann FX-60-157 airfoil shape, frequently used on sailplanes and occasionally in rotorcraft. Internally, the structure was assumed to consist of a thick skin with a wing spar toward the quarter chord. The unmodified airfoil structure contains a sharp and thin trailing edge that was difficult to make sufficiently stiff for the purpose of a realistic deployable flap simulation, so the trailing edge was blunted to avoid overly complicating the interpretation of the results.

Flight conditions are approximately that at sea level. The structure is flying at a Mach number of 0.35 and an ambient temperature of 300 K at atmospheric pressure. The chord length of the flap is 1.0 meter.

3. Numerical Model and Procedure

There are three important aspects to accurately modeling an aeroelastic deployable structure. First, a validated and trusted structural model is obviously required to begin the analysis. The structure for the considered demonstration case was modeled with the 6.14-1 release of Abaqus/Standard (SIMULIA, 2014). Abaqus/Standard was responsible for computing the structural response and the deployment schedule of the structure. An intentionally coarse mesh was constructed for the purely notional geometry considered in these analyses, although it should be emphasized that, like most simulations, application of this methodology to existing physical problems will only be as accurate as the least-accurate model. The second important part of the aeroelastic model is the simulation of the fluid dynamics. In these analyses, the commercial CFD code Star-CCM+ (CD-Adapco, 2014) was used to model the fluid domain. Once again, an intentionally coarse mesh was used to discretize the domain; however, application to aeroelastic problems where accuracy is crucial would benefit from a finer mesh. The CFD mesh used in these demonstrations ran efficiently on a single twelve-core desktop computer; finer meshes could be run on a small computer cluster. The last component of the numerical model is linking the solid and fluid domains. This was accomplished with SIMULIA's Co-Simulation Engine (CSE). The CSE allows for communication of aerodynamic loads and displacements between the two domains. Critically, the two domains do not need to be point matched at the interface, as the CSE is capable of performing the required interpolation between domains while conserving energy.

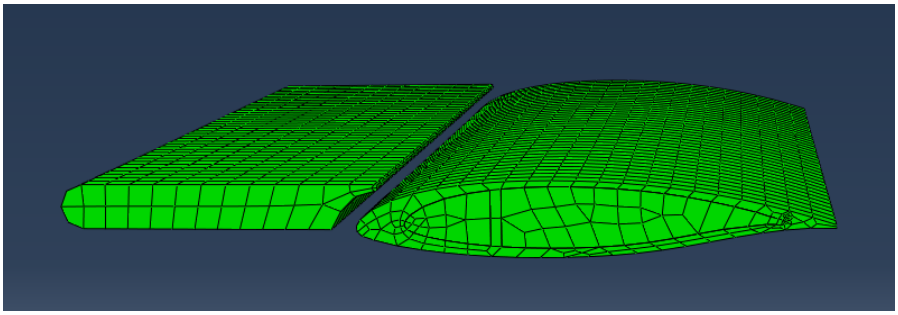

Figure 3. The FEM mesh was largely composed of continuum elements, with shell elements on the flap sides.

The FEM mesh, depicted in Figure 3, consisted of 4,960 eight-node continuum elements with reduced integration with material properties corresponding to aluminum. It is necessary to have a watertight mesh geometry to couple with the fluid dynamic solver, so an additional 85 shell elements were applied to the flap to seal off the hollow inside. Two connector elements (depicted in Figure 4) attached the leading slat to the trailing flap, with the ends of the connectors attached to the surrounding structural mesh with `*COUPLING *KINEMATIC` elements. Commanded motions in these connectors actuated the deployment of the flap.

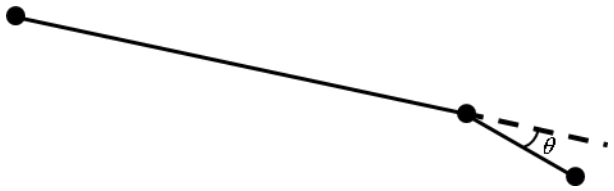

Figure 4. A schematic of the two connectors, with free play angle, θ.

Free play in the actuators was obtained by applying a simple nonlinear model to the connector elasticity, as shown in Figure 5. As illustrated, there was no load over a one-degree region of free play, after which the loads increased sharply. For studying an existing free-play problem, one would want to measure the free play response in the device by applying deflections in both directions and then measuring the loads to get the problem-specific response.

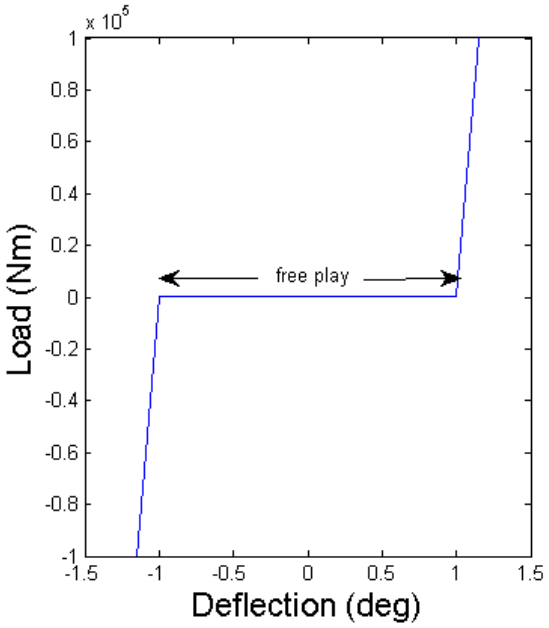

Figure 5. Free play was modeled as a region where a change in deflection could be obtained without maintaining a supporting load.

The fluid dynamics were resolved with Star-CCM+ (version 9.06.009). The use of relative body motion was accomplished using overset grids. The leading slat was made a part of the stationary background grid, while the flap grid was allowed to move freely as an overset mesh. Star-CCM+ largely handles the overset process, computing fringe points for interpolation between the two meshes automatically. Large body motion did require the use of the in-built "alternative" hole-cutting scheme, which is more robust for close bodies, as well as resetting the mesh motion to zero to avoid negative Jacobians in the refined boundary layer.

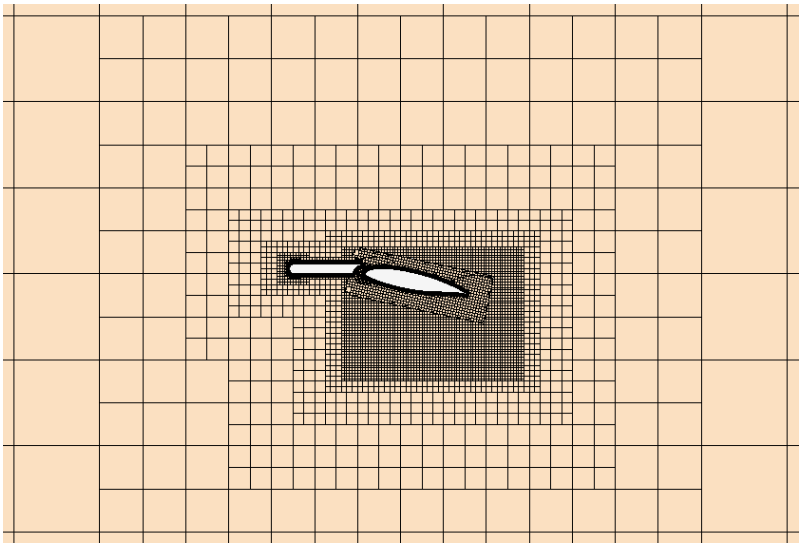

Figure 6. The CFD domain was composed of two overset meshes. The large background mesh contains the leading slat while the flap is contained in the small overset mesh.

Both domains were meshed with hexahedral template cells, similar to an octree approach (Figure 6). The near-body meshes contained fifty prismatic cell layers to aid in capturing the boundary layer with a stretching ratio of 1.2. As with any viscous CFD calculation, it is best to verify that the wall y+ value at the first grid point is less than 1 in order to adequately resolve the boundary layer. As observed in Figure 7, this condition was satisfied for the current conditions. If conditions were varied, for example upstream dynamic pressure, it would be necessary to check wall y+ again.

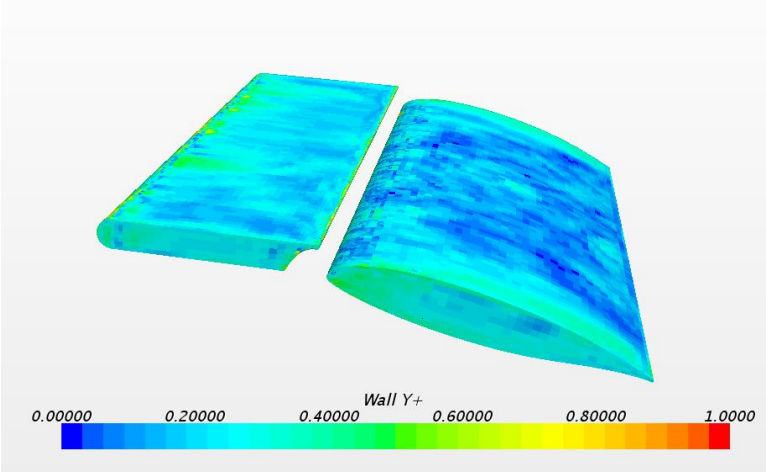

Figure 7. Wall y+ values indicate appropriate initial wall spacing (y+ < 1).

The Menter k-omega SST (Menter, August 1994) detached-eddy turbulence model was employed in these calculations. Increased refinement of the CFD meshes will further help resolve separated flow physics as the computations incorporate increasingly more LES modeling.

Simulations were performed with one-millisecond time steps in Star-CCM+. Temporal discretization was limited first-order, and five subiterations were applied to converge the flow variables. Coupling between Star-CCM+ and Abaqus/Standard was performed explicitly at one-millisecond intervals.

Before coupling began, the CFD calculations were performed with rigid bodies without motion to allow nonphysical transients to leave the domain. After the solution became steady, Abaqus/Standard was coupled with only elastic deformation included in the initial solution (i.e., without large body motion). The objective of this step is to avoid nonphysical excitement of the structure at the start of the deployment. To improve computational efficiency of this step, the structure was solved with a quasi-static approach that did not include inertial terms. This was done until a steady response was obtained, indicating that the system was ready for the deployment maneuver.

It should be noted that using the coarse meshes applied in this study, the computational cost was dominated by the CFD calculations, and less than 1% of the run time was attributed to the structural computations. Thus, while rigid, moving body simulations can be performed, the added cost of coupling to Abaqus/Standard may be insignificant while providing insight into the aeroelastic characteristics of a structure.

The deployment of the flap was computed with a dynamic structural analysis (therefore including the inertial terms). As previously discussed, resolving the inertial response was an important objective of this work. These computations were performed with and without free-play effects. Comparisons to quasi-static analysis results were also made.

While the stability margins were not calculated in this effort, they are readily possible with this methodology. To compute these modal parameters, one would vary the dynamic pressure for a given free-play amount. An instability would be immediately apparent as a divergence of the solution, enabling flutter or divergence speeds to be determined. Actual computation of the frequency and damping requires additional analysis. As an example, see Bauchau and Wang's partial Floquet analysis for large multibody systems (Bauchau & Wang, October 2007), which is well-suited to these types of computations (Zaki, et al., May 2010).

4. Demonstration Results

The described dynamic analysis procedure was compared to the quasi-static procedure where no large body motion was included. Perhaps surprisingly, the dynamic response was, in fact, less computationally expensive to obtain than the quasi-static response. This is because the goal of a quasi-static analysis is an approximately steady result, which took more iterations to achieve. The computational cost per iteration between the cases was approximately the same, as both used the same meshes and the same codes. The dynamic analyses, however, only required that the deployment maneuver be completed and were on average approximately four times faster to produce than each quasi-static analysis. Furthermore, several quasi-static analyses were required at each deployment angle while the dynamic analysis swept through all deployment angles in one simulation. Thus, despite the additional complications associated with the moving geometry, the dynamic analyses were considerably easier to obtain than the traditional quasi-static analyses.

The results of these analyses are depicted in Figure 8 and indicate that the dynamic loads tend to oscillate about the mean of the quasi-static analysis. These amplified loads are imparted to the actuator and surrounding structure and should be considered during a fatigue life assessment.

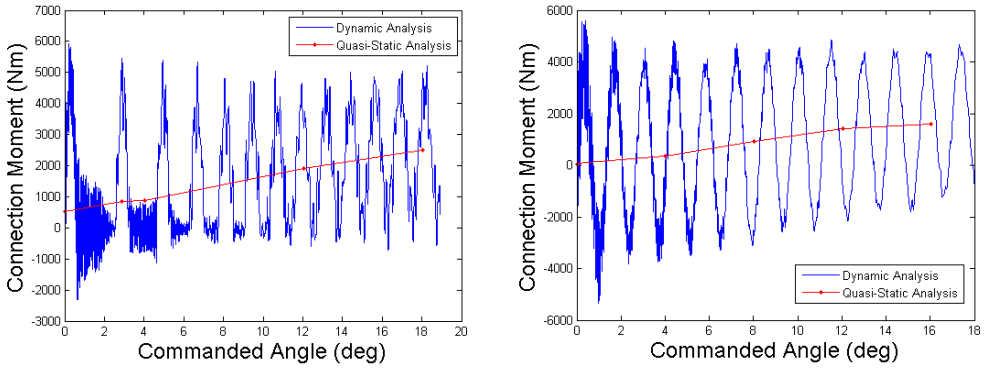

Figure 8. The results comparing dynamic (blue) and quasi-static (red) analyses. Left: one degree of free play is included. Right: no free play is included.

It is useful to compare the effects of free play in Figure 8. With free play included, the moment peaks and then decays, followed by another peak that repeats for the first ten degrees. This is attributed to the flap impacting the stop at the end of the free play region, exciting the structure, which then rings out. This is confirmed in Figure 9, which reveals that the actuator connector

comes to near-rest at the free-play stop toward the end of the simulation. It is thus unsurprising that this impact behavior is entirely missing from the case where free play is not included, and that instead a dynamic oscillation about the mean quasi-static loading occurs.

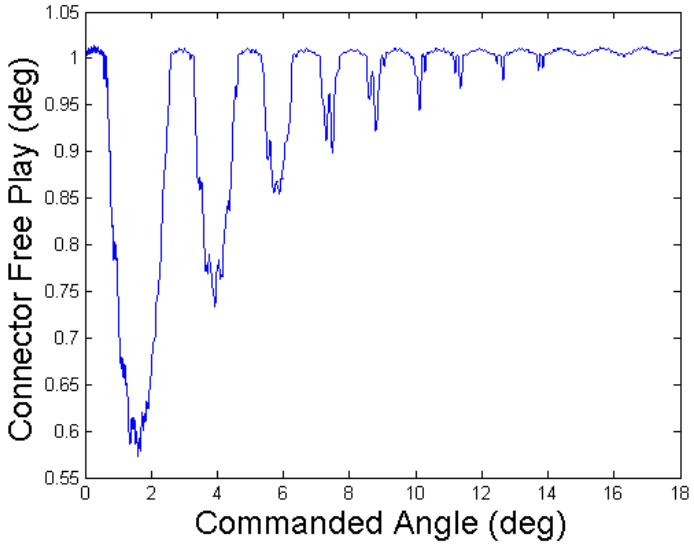

Figure 9. The actuator connector angle as a function of commanded angle.

Examination of the frequency response of the free play (Figure 10, left image) indicates an excitation frequency of approximately 30 Hz. Performing a modal analysis within Abaqus/Standard of the initial position indicates that the first mode is a flap-only rigid body mode, followed by a mode at approximately 88 Hz. The inability to reproduce the dominant mode in the response is due to the linear nature of the eigenvalue/eigenvector modal approach. Removing the free play and repeating the analysis (modal response shown in Figure 11) indeed reveals the first mode is 29.9 Hz, as expected.

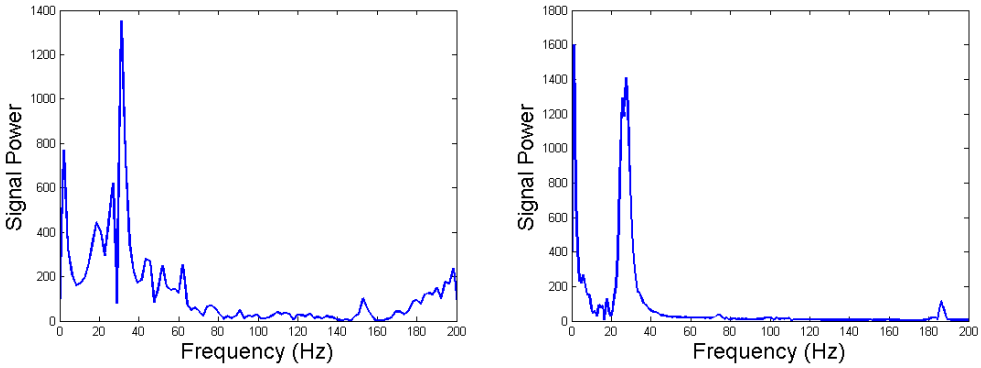

Figure 10. Frequency response of the dynamic analysis with free play (on left) and without free play (on right).

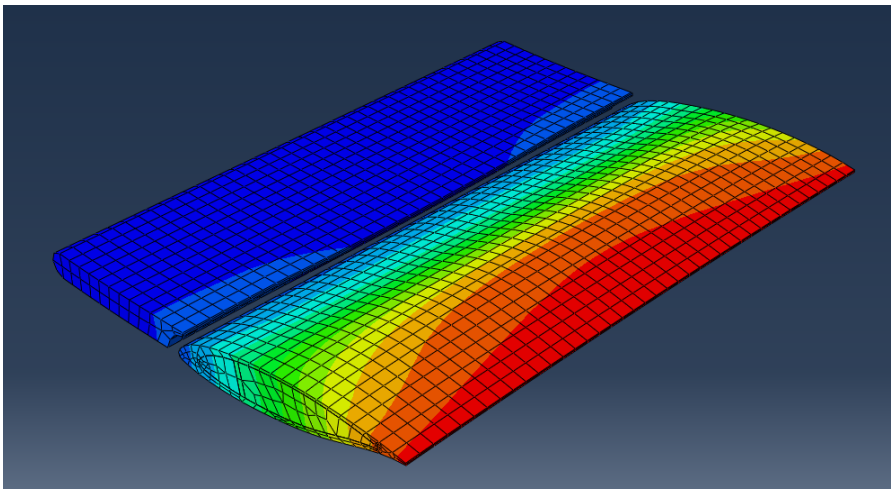

Figure 11. The first mode of the demonstration case when no free play is included.

Since the quasi-static analyses did not include inertial terms, it is possible to apply a single-pole low-pass filter at the first modal frequency of 30 Hz to the dynamic results and compare the results of the procedures again. Doing this (illustrated for results both with and without free play in Figure 12) removes the modal excitation and allows additional comparisons to be drawn. It is clear that the case with free play (Figure 12 left) does in fact contain the quasi-static response despite this not being apparent in the unfiltered signal (Figure 8 left). While the case without free play clearly follows the same trend before filtering, the application of the low-pass filter does aid in reducing the magnitude of the excitation and follows the same trend as the case without free play. This suggests that for certain classes of problems, a time-accurate dynamic analysis could supplant multiple quasi-steady simulations.

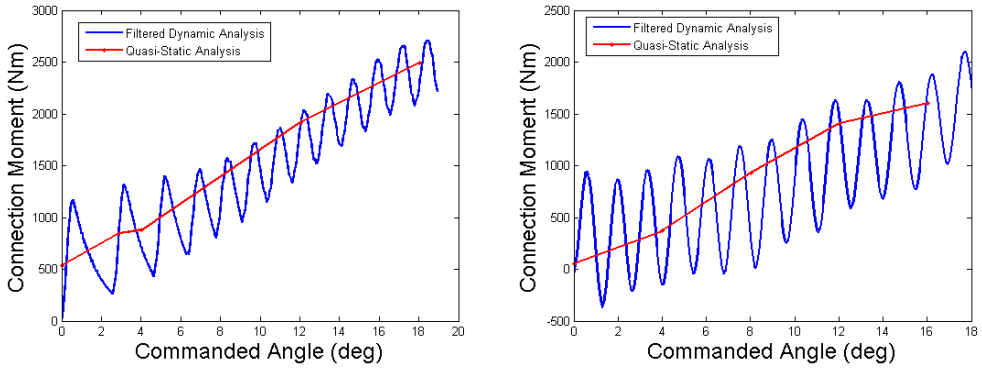

Figure 12. Results of the dynamic analysis after a low-pass filter of 30 Hz is applied are compared to quasi-static results both with free play (left) and without free play (right).

One key implication of performing the time-accurate deployment simulation is the discovery of the magnitude of the oscillatory load on the actuator, which may be critical for fatigue life assessments.

5. Conclusions

The following conclusions may be drawn:

- A practical methodology for performing free-play analyses on aeroelastic deployable structures has been demonstrated.
- The effect of free play on dynamic loads may significantly exceed the loads predicted by a quasi-static analysis. This is attributed to the dynamic impact of the flap on the actuator as it transitions through the region of free play.
- The time-accurate deployment simulation enables a prediction of the magnitude of oscillating loads, which is required when determining the fatigue life of the relevant components, whereas quasi-static simulations could only predict the mean stress.
- Dynamic analyses may be performed at reduced computational costs compared to the quasi-static analyses. This is because the quasi-static analyses attempt to produce a steady solution where the transients have left the modeled system, which may require simulation times that exceed the time of deployment.
- A single dynamic analysis may be used with a low-pass filter below the first modal frequency to obtain results similar to quasi-static simulations.
- The described methodology is well suited for aeroelastic stability margin calculations through standard time-accurate stability procedures. Doing so requires varying the problem's relevant parameters such as the freestream dynamic pressure and the amount of free play to determine stability.

6. Acknowledgements

The authors would like to thank Dr. Eric Blades of ATA Engineering, Inc., for suggesting this type of analysis, as well as for discussions regarding the computation of aeroelastic stability margins.

7. References

Bauchau, O. & Wang, J., October 2007. Efficient and Robust Approaches to Stability Analysis of Large Multibody Systems. *Journal of Computational and Nonlinear Dynamics,* 3(1).
Blades, E. & Cornish, A., January, 2015. *Aeroelastic Stability Predictions of a Business Jet Landing Gear Door Using High Fidelity Fluid-Structure Interaction Tools.* Kissimmee, FL.
CD-Adapco, 2014. *Star-CCM+ 9.06.009 User's Manual*.
Federal Aviation Administration, October 2014. *Aeroelastic Stability Substantiation of Transport Category Airplanes,* No. 25.629-1B.
Menter, August 1994. Two-Equation Eddy-Viscosity Turbulence Models for Engineering Applications. *AIAA Journal,* 32(8), pp. 1598-1605.
Mitcheltree, R., Salas, M. & Hassan, H., 1988. Grid embedding technique using Cartesian grids for Euler solutions. *AIAA Journal,* 26(6), pp. 754-756.
Noack, R., June 2007. *A Direct Cut Approach for Overset Hole Cutting.* Miami, FL.
SIMULIA, 2014. *Abaqus 6.14 User's Manual*.
Tang, D. & Dowell, E., November 2011. Aeroelastic Response Induced by Free Play, Part I: Theory. *AIAA Journal,* 49(11), pp. 2532-2542.
Zaki, A., Reveles, N., Smith, M. & Bauchau, O., May 2010. *Using Tightly-Coupled CFD/CSD Simulations for Rotorcraft Stability Analysis.* Phoenix, AZ.

8. Appendix

Simulations were performed on a Hewlett-Packard Z420 desktop computer containing the Intel® Xeon® CPU E5-1650 with a clock speed of 3.20 GHz and 32.0 GB of RAM. Eight cores were used in each simulation. Dynamic simulations required 208 CPU-hours while quasi-static simulations each required between 168 and 376 CPU-hours. Abaqus/Standard alone required approximately just one CPU-hour.